Iron — silver oxide nanoadsorbent synthesized by co-precipitation process for Fluoride removal from aqueous solution and its adsorption mechanism

Article *in* RSC Advances · October 2015

DOI: 10.1039/C5RA17595J

CITATIONS
29

READS
332

6 authors, including:

Roshanak Rezaei Kalantary
Iran University of Medical Sciences
150 PUBLICATIONS **1,669** CITATIONS

SEE PROFILE

Babak Kakavandi
Alborz University of Medical Sciences
80 PUBLICATIONS **1,669** CITATIONS

SEE PROFILE

Ehsan Ahmadi
Tehran University of Medical Sciences
45 PUBLICATIONS **522** CITATIONS

SEE PROFILE

Research Article

Received: 9 February 2016 Revised: 21 March 2016 Accepted article published: 5 April 2016 Published online in Wiley Online Library: 10 June 2016

(wileyonlinelibrary.com) DOI 10.1002/jctb.4990

Magnetic adsorption separation process: an alternative method of mercury extracting from aqueous solution using modified chitosan coated Fe_3O_4 nanocomposites

Ali Azari,[a,b*] Hamed Gharibi,[c] Babak Kakavandi,[d] Ghader Ghanizadeh,[e] Allahbakhsh Javid,[c] Amir Hossein Mahvi,[b] Kiomars Sharafi[a,b] and Touba Khosravia[f]

Abstract

BACKGROUND: In the present work, Hg (II) is considered as one of the most dangerous elements being released excessively into the environment from various sources. Therefore, the aim of this study is the removal of Hg (II) from wastewater effluent by synthesizing a magnetic chitosan modified with glutaraldehyde (MCS-GA) as an adsorbent. The composite structure was characterized using SEM/EDAX, FTIR, and XRD techniques. The adsorbent was tested by a batch system to determine the optimum conditions for removing Hg (II) under real conditions.

RESULTS: The results showed that 0.5% GA effectively enhanced the removal efficiency. The maximum adsorption capacity of MCS-GA was 96 mg g^{-1} at pH 5.0 and 25 °C. The adsorption isotherm data obeyed the Langmuir model (R^2>0.981) and pseudo-second-order (R^2>0.996) kinetic models. It was also found that Hg (II) adsorption on MCS-GA is inherently exothermic and occurs spontaneously. The reusability of MCS-GA was approved over 12 sequential cycles of adsorption–desorption. ANOVA analysis showed that the contact time has a synergistic effect on Hg (II) removal, whereas pH and initial concentration have antagonistic effects.

CONCLUSION: Overall, the synthesized adsorbent was able to remove Hg (II) efficiently under both experimental and real conditions.

Supporting information may be found in the online version of this article.

Keywords: magnetic chitosan; cross-linking; hg (ii); biosorption; RSM approach

INTRODUCTION

For many decades, the excessive release of heavy metals into both surface and ground water resources has raised serious concerns among researchers around the world.[1] These elements are inherently non-biodegradable and can accumulate in soil and plants and bio-accumulate in organisms and the human body. In other words, these compounds are toxic and can directly and/or indirectly affect the ecosystem.[2] Among these compounds, Hg (II) is one of the most dangerous elements. This is mainly due to its properties of solubility and stability, bioaccumulation, long-term residence times at low concentrations, and high toxicity; thus researchers have paid much attention to this element.[3] The chemical industry, burning fossil fuels and inappropriate discharges from anthropogenic activities are the major sources of mercury release into the environment.[4] Various studies have predicted that mercury emissions would reach 4860 Mg worldwide in 2050; it is noteworthy that this amount was 2480 Mg in 2006.[5] Furthermore, recently conducted studies have firmly proved that intakes

* *Correspondence to: A Azari, Department of Environmental Health Engineering, School of Public Health, Tehran University of Medical Sciences, Tehran, Iran. E-mail: azari.hjh@gmail.com*

a *Department of Environmental Health Engineering, School of Public Health, Kermanshah University of Medical Sciences, Kermanshah, Iran*

b *Department of Environmental Health Engineering, School of Public Health, Tehran University of Medical Sciences, Tehran, Iran*

c *Department of Environmental Health Engineering, School of public Health, Shahroud University of Medical Sciences, Shahroud, Iran*

d *Department of Environmental Health Engineering, School of Public Health, Ahvaz Jundishapur University of Medical Sciences, Ahvaz, Iran*

e *Health Research Center, Baqiyatallah University of Medical Sciences, Tehran, Iran*

f *Research Center for Environmental Determinants of Health (RCEDH), Kermanshah University of Medical Sciences, Kermanshah, Iran*

of Hg (II) more than the standard level cause serious cognitive and motion disorders, and also impair renal function, reproductive organs, liver, hepatic, and the central nervous system.[6] Therefore, it is essential to develop an effective and economical technology to remove released Hg (II) from the environment.

Over the years various methods have been proposed. One of the most recognized and widely used methods is the adsorption process.[7] This is a cost-effective process with high efficiency and easy operational features.[8] Since the performance and efficiency of an adsorption process is strongly dependent on the adsorbent features, synthesis of adsorbents with high sorption capacity and affinity for Hg (II) is a considerable challenge.[9] Moreover, the reversibility and regeneration abilities of a synthesized adsorbent should also be taken into account. Adsorbents comprised of natural polymers could be widely used in removing heavy metal ions from water or wastewater.[10] Accordingly, polysaccharides-based glucosamine, particularly chitosan (CS), have been widely studied. Previous studies reported that chitosan alone is not suitable as a bio-sorbent to remove high concentration pollution.[11] In order to overcome this issue, a cross-linked process has been suggested to modify the physical characteristics (i.e. porosity, functional groups and resistance against solubility) of chitosan.[3,12] Crosslinking chitosan with bifunctional reagents such as glutaraldehyde (GA), epichlorohydrin (ECH), ethylenediamine tetra acetic acid (EDTA), and polyvinyl alcohol (PVA) has been reported in the literature.[13] Glutaraldehyde or 1, 5-pentanodial has been commonly used in cross-linking and protein immobilization procedures through Schiff's base reaction between aldehyde groups and amino groups in the CS structure. CS-GA is a cheap and convenient method to promote fixation and is known as a strong chelating agent for Hg (II).[14]

However, the separation and recovery of CS-GA from treated water by the usual methods such as filtration or centrifugation are not possible, causing loss of the adsorbents and creating secondary pollutants. The application of a magnetic bio-sorbent to solve the separation/recovery problems is considered in our study. Therefore in the present work magnetic properties were added to sorbents using Fe_3O_4 as a source of iron to facilitate phase separation of magnetic chitosan–glutaraldehyde (MCS-GA) by an external magnetic field. Further, magnetic separation techniques are more amenable to automation. In this study, the MCS-GA was characterized as a sorbent by X-ray diffraction (XRD), scanning electron microscopy (SEM), transmission electron microscopy (TEM), Fourier transform infrared (FTIR) spectroscopy, energy-dispersive X-ray (EDX) spectroscopy, Brunauer–Emmett–Teller (BET) method, and vibrating sample magnetometer (VSM) techniques.

EXPERIMENTAL

Chemicals

Ferric chloride hexahydrate ($FeCl_3.6H_2O$, 97%), Ferrous chloride tetrahydrate ($FeCl_2.4H_2O$, 98%) were purchased from Merck Company and used without further purification. Hydrochloric acid (HCl, 35–37%) and sodium hydroxide (NaOH, 93%) solutions were utilized to adjust pH values during the experiments. Glutaraldehyde ($OHC(CH_2)_3CHO$, 25% in H_2O) and acetic acid (CH3CO2H, ≥99%) were obtained from Sigma-Aldrich. Hg (II) stock solution was prepared using mercury (II) chloride ($HgCl_2$, 99% Sigma-Aldrich). A pH meter (Hach-HQ-USA) and incubator shaker (VWR 1535) were used to measure the pH of solutions and adjust temperature and stirring rate, respectively. All chemicals used were of analytical grade.

Table 1. XRF analysis of shrimp shells

Chitin source	shrimp shells	Chitin source	shrimp shells
Ca (mg L^{-1})	**751.1**	Fe(mg L^{-1})	**1.89**
K (mg L^{-1})	**16.73**	CaCO3 (%)	**50.03**
Na (mg L^{-1})	**40.23**	Protein (%)	**27.84**
Mg (mg L^{-1})	**45.93**	Chitin (%)	**22.13**

Synthesis and characterization of MCS-GA

Shrimp shells (Jinga shrimp family) were purchased in Iran. They were washed, dried and screened through a 200-mesh sieve; then the chitin and chitosan were extracted and prepared, using demineralization and deproteinization, respectively.

Chitin extraction

The demineralization (i.e. separating the inorganic matter) was done by immersing 50 g of screened shells in diluted water/HCl solution (10% w/w) for 6 h. Then, the shells were filtered and washed using deionized water to reach neutral condition. In order to conduct the deproteinization step, the demineralized shrimp shells were immersed in diluted water/NaOH solution at 70 °C for 1 day. Then, residual impurities were filtered and washed. Finally, to obtain the decolorized and pure chitin, it was washed consecutively with acetone and hot ethanol, and dried at 40 °C for 8 h. Table 1 shows the XRF results for the shrimp shells.

Preparation of CS

In this study chitosan was extracted using the deacetylation method of Younes *et al.*[15] Also water/NaOH (50% w/w) at 100 °C was used for 24 h to treat the extracted chitin sample, and then, the sample was dried in an oven. To purify the basic chitosan, all chitosan samples were kept in 3% acetic acid and then 20% NaOH solution. Finally, chitosan was washed to reach the neutral form and then freeze-dried at −70 °C (i.e. lyophilized).

Synthesis of MCS

Chitosan supported iron oxide was synthesized by a co-precipitation method described by Roth *et al.*[16] Predetermined quantities of ferric and ferrous chlorides (molar ratio 2:1) were dissolved in 200 mL of distilled water. Then, 10 g of chitosan was added to the solution on a heated mechanical stirrer (70 °C and 250 rpm) and left for 3 h. Sodium hydroxide solution (70% V/V) under vigorous stirring was added in a dropwise process into the resulting Fe^{2+}–chitosan solution. During the reaction process a pH of 11 was recorded. After the reaction, the black beads were separated from the NaOH solution by external magnet and washed to remove the impurities and soluble salts. The beads were then dried at 75 °C for 12 h and calcined at 400 °C for 6 h. The calcined beads were cooled at room temperature and stored in a desiccator.

Synthesis and characterization of MCS-GA

Grafting of amine and hydroxyl groups using glutaraldehyde (crosslinking agent) was performed according to the method applied by Sargin *et al.*[17] 8 g of modified chitosan beads were dissolved in 100 mL of acetic solution (5%) to produce a final concentration of 2% (w/v). In distinct flasks, 25% (w/w) of GA solution (31.2 mmol) was prepared at 333 K. Subsequently, the contents of the GA solution flask were added to the MCS solution and stirred

Table 2. Analysis techniques used to characterize adsorbents

Techniques	Instrument model	Application
SEM	PHILIPS, S360, Mv2300	To study the morphological and surface texture properties
TEM	PHILIPS, EM 208 S 100KV	To study the particles size, shape and size distribution
XRD	Quanta chrome, NOVA2000	To study the phases and crystalline structure
VSM	Lakeshore 7307	To study the Magnetic properties
EDX	PHILIPS, S360, Mv2300	To study the elemental composition
FTIR	FTS-165, BIO-RAD, USA	To study the information of various function groups in the adsorbent
N_2 Sorption/desorption	NOVA 2200 - Quantachrome	To study the specific surface area and pore structure

Table 3. Independent variables and their levels used in the experimental design

			Level (coded value)		
Variable	Symbols	Units	−1	0	+1
pH	A	-	2	5	8
Contact time	B	min	10	50	90
Initial concentration	C	Mg L^{-1}	25	65	100

at 70 °C for 8 h until the mixed solution reach a homogenous condition. 50 mL of NaOH (1 mol L^{-1}) was added to form a MCS-GA slurry sample, and mixed for 4 h at 333 K to raise its pH level to 9. During these processes, the pH of solutions was kept at this level. The slurry mixture was separated from solution using an external magnet, and then dried in a vacuum oven at 353 K. The solid product was ground and sieved to obtain a uniform adsorbent (Scheme S1). Table 2 indicates the summarized techniques applied for characterizing the MCS-GA bio-sorbent.

Sorption experiments

Optimizing the experimental design

To optimize the process, response surface methodology and statistical analysis were applied. Design-Expert software V. 8.0 (Stat-Ease Inc., Minneapolis MN, USA) based on a Box-Behnken design (BBD) was used to investigate the effects of independent variables on Hg (II) removal efficiency; these variables are listed in Table 3. A three-factorial BBD was used to optimize the Hg (II) adsorption process by MCS-GA. The applied Box-Behnken design (BBD) is presented in detail in the Supplementary material.

Batch experiments

The Hg (II) stock solution was prepared by dissolving an exact amount of $HgCl_2$ in 1000 mL of deionized water. Hg (II) sorption experiments in batch condition were conducted using 100 mL Erlenmeyer containers in which 50 mL of the solution was added; a shaker was utilized at 180 rpm to ensure ideal mixing. pH of 2–8, GA loading of 0–1 mol L^{-1}, Hg (II) concentration of 25–100 mg L^{-1} and contact time of 0–50 min were considered in the present work. After the adsorption process and using a magnet to separate the bio-sorbent, the remaining Hg (II) concentrations <1 and > 1mg L^{-1} were measured by atomic fluorescence spectroscopy (AFS9130, Titan Instruments, Tehran, Iran) and inductively coupled plasma optical emission spectroscopy (ICP-OES, Prodigy, University of Science and Technology, Tehran, Iran), respectively. All experiments were repeated and the average values of results are reported. An equilibrium adsorption capacity of adsorbent (q_e) and removal percentage (%) were calculated according to the Equation (1) and (2):

$$q_e = \left(\frac{C_0 - C_e}{m}\right) \times v \quad (1)$$

$$r\,(\%) = \frac{C_{des}}{C_{ads}} \times 100 \quad (2)$$

Here, C_0 (mg L^{-1}) and C_e (mg L^{-1}) are initial and final Hg (II) concentrations, respectively; V is the volume of solution (L) and M the weight of used bio-sorbent (g). The zeta potential of adsorbents was measured using a Zeta Potential Analyzer (ZA500, USA). For calculating the zeta potential, the samples were diluted with 0.2 mmol L^{-1} sodium chloride solution at pH 2–11 and measured in the automatic mode.

MCS-GA reusability and Hg (II) Desorption

To determine the reusability of MCS-GA, 12 cycles of sequential adsorption–desorption were carried out. Each adsorption process was performed in batch mode with Hg (II) initial concentration of 50 mg L^{-1} for 6 h. Afterwards, the MCS-GA was separated from the sample using the external magnetic field, and washed lightly with distilled water to remove the adhered solution. For the desorption process, the collected adsorbent was immersed in 20 mL of 0.5 mol L^{-1} HCl at 25 °C for 1 h while it was being rigorously stirred. To determine Hg (II) desorption, the samples were taken from the supernatant. It can be noted that the regenerated adsorbents were washed several times with DI water before the next cycle.

RESULTS AND DISCUSSION

Characterization of MCS-GA

SEM images of pure Fe_3O_4 nanoparticles and CS, are shown in Fig. 1(a) and 1(b). According to the figures, the pure Fe_3O_4 is formed in a compact and ball-like shape with a diameter of about 30 nm; CS is in the form of nanoflakes of size range 50 to 200 nm. As shown in Fig. 1(c), MCS has a spherical shape with a smooth surface; but, when modified with GA to formed MCS-GA, the shape becomes irregular and it aggregates because of the grafting reaction of MCS with GA (Fig. 1(d)). According to the SEM micrograph, Fe_3O_4 nanoparticles became immobilized on the surface of CS with a core–shell structure and an average MCS-GA diameter of about 45 nm. Comparing Fig. 1(d) with 1€, it is obvious that the surface of the magnetic modified chitosan has a rough structure as well as good porosity, which is suitable for mass transfer of Hg (II) ions; however, after adsorption, drastic changes occurred at the surface of the adsorbent resulting in a high rate of bonded crystals on the surface. The SEM images indicate that Hg (II) ion was adsorbed

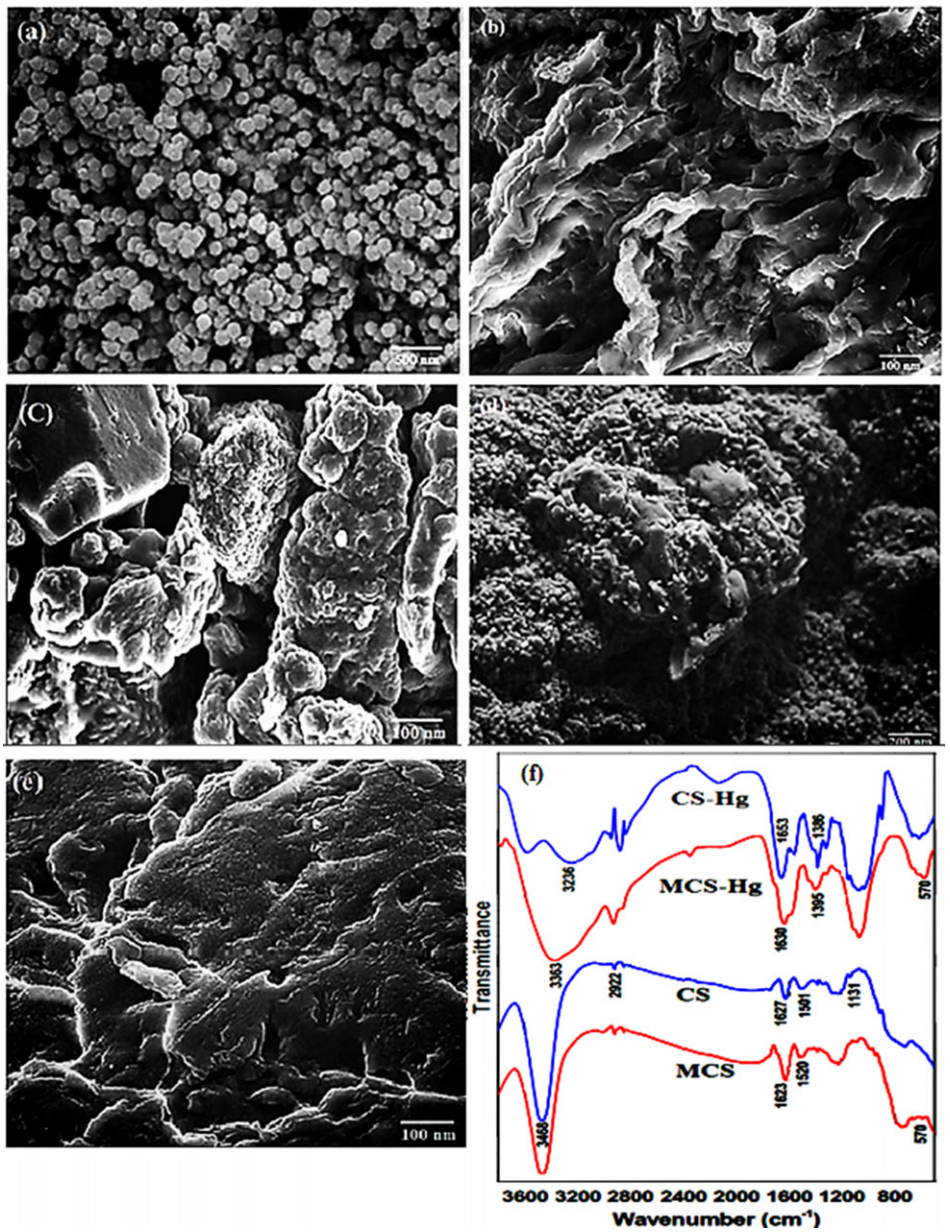

Figure 1. SEM images of: (a) Fe_3O_4 NPs; (b) CS; (c) MCS; (d) MCS-GA; (e) MCS-GA-Hg; (f) FT-IR spectra of pristine and modified CS before and after adsorption.

by the pores of MCS-GA, developing a layer of Hg (II) on its surface.

The result of FTIR analysis is shown in Fig. 1(f), with a peak at 3468 cm^{-1} in the chitosan spectrum observed before the adsorption process; this could be due to the stretching vibration of O—H, the extension vibration ofN—H, and the inter-hydrogen bonds of the polysaccharide .[18] In addition, the C = O stretching vibration mode of amide I (NHCO) along withN—H deformation and bending of the NH group could be the reason for characteristic bonds observed at 1627 and 1501 cm^{-1} (1520 cm^{-1} in MCS), respectively. The C—H, C—N (amino group bond), and hydroxyl group stretching vibrations manifested themselves through the peaks at 2922 cm^{-1}, 1217 and 1096 cm^{-1}, respectively. Other characteristic bonds appeared at 1131 cm^{-1}, 1028 cm^{-1} and also both 1060 cm^{-1} and 1015 cm^{-1} result from (1–4)–glucosidic bond in polysaccharide, C-O–C in the glucose circle and CH—OH in cyclic compounds.[19] A new peak at 570 cm^{-1} was observed in the MCS spectrum, which could be due to the Fe–O group; in other words, it demonstrates that iron oxide (Fe_3O_4) nanoparticles are successfully deposited on the CS. This result is in agreement with the data reported in previous studies.[4,20]

After the adsorption process, the intensity of the peak related to the —NH group in amine is reduced; this verifies that N_2 atoms are the main sites for mercury adsorption on MCS-GA. Based on the results, peaks at 1627 and 1623 cm^{-1} shift to 1653 and 1630 cm^{-1}, respectively, after the adsorption process, reflecting the formation of Hg (II) chelate with nitrogen atoms of amino groups (–NHCO). Furthermore, new bands at 1386 cm^{-1} and 1395 cm^{-1} appeared in CS—Hg (II) and MCS—Hg (II), respectively, and this could be due to C—N stretching vibration occurring after the cross-linking process.[21] Imine bond (i.e. structure resulting from preliminary reaction between amino and GA) is capable of adsorbing cationic metals, including Hg (II).[22] Moreover, the strong peak related to OH-groups at 3468 cm^{-1} changes to 3236 cm^{-1} and 3363 cm^{-1} in

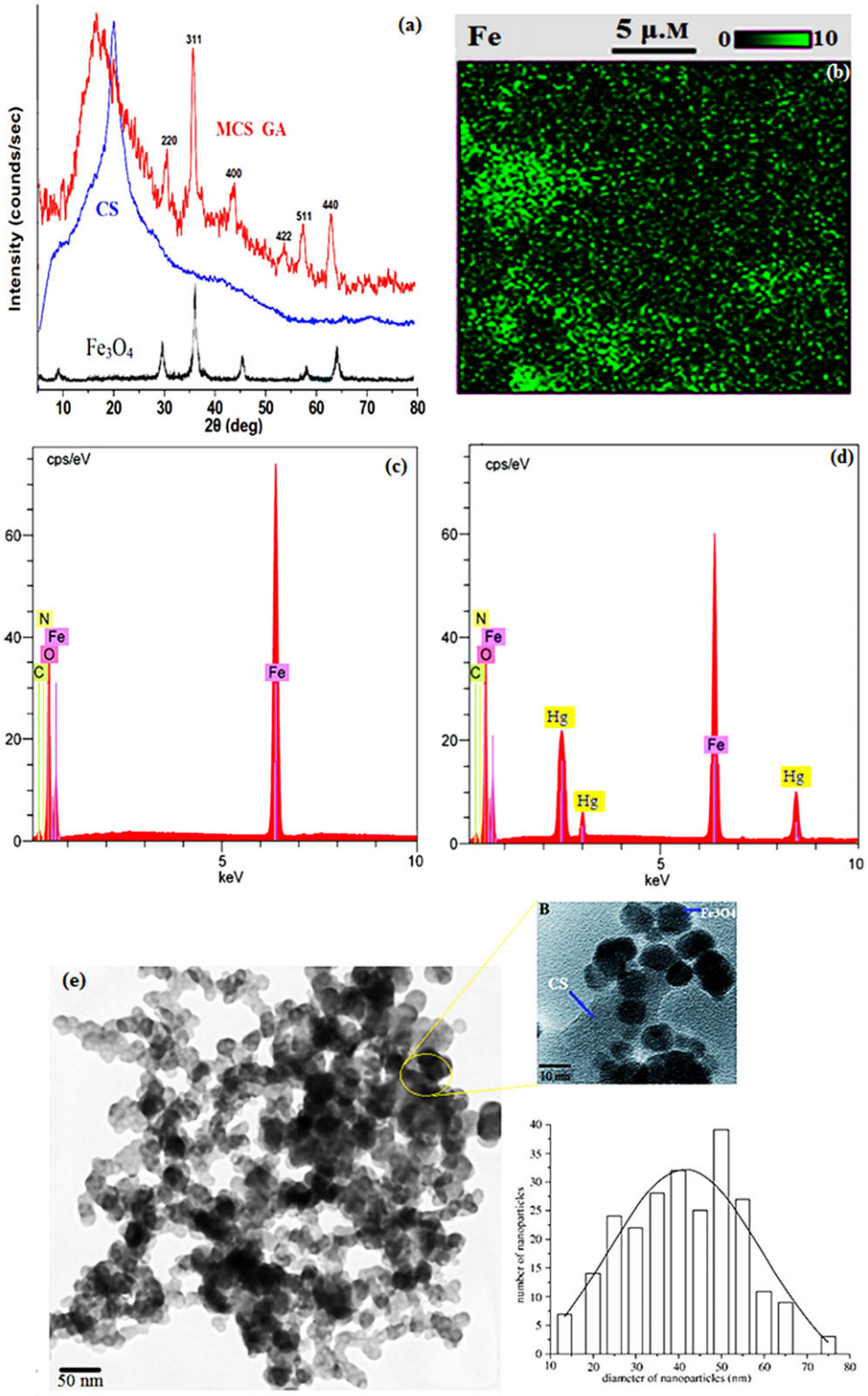

Figure 2. (a) XRD patterns of Fe_3O_4 NPs, CS, and MCS-GA; (b) EDX mapping of MCS-GA. EDX spectrum of MCS-GA before (c) and after (d) adsorption, and (e) TEM images of modification of the CS.

CS—Hg (II) and MCS—Hg (II), respectively, clearly indicating that –OH groups can positively influence the sorption process. Yuwei *et al.*[20] reported that the —OH and —NH are the main agents in the adsorption process. Scheme 1 shows the chelated structures of Hg (II) with MCS-GA.

The XRD patterns of pure forms of Fe_3O_4, CS and MCS-GA are shown in Fig. 2(a). X-ray diffraction spectrogram in 2θ equates 20.2°, related to the structure of chitosan. Six characteristic peaks at $2\theta = 30.1^{\circ}, 35.5^{\circ}, 43.3^{\circ}, 53.4^{\circ}, 57.2^{\circ}$, and 62.5°, which are marked by 220, 311, 400, 422, 511, and 440 indices, respectively, are

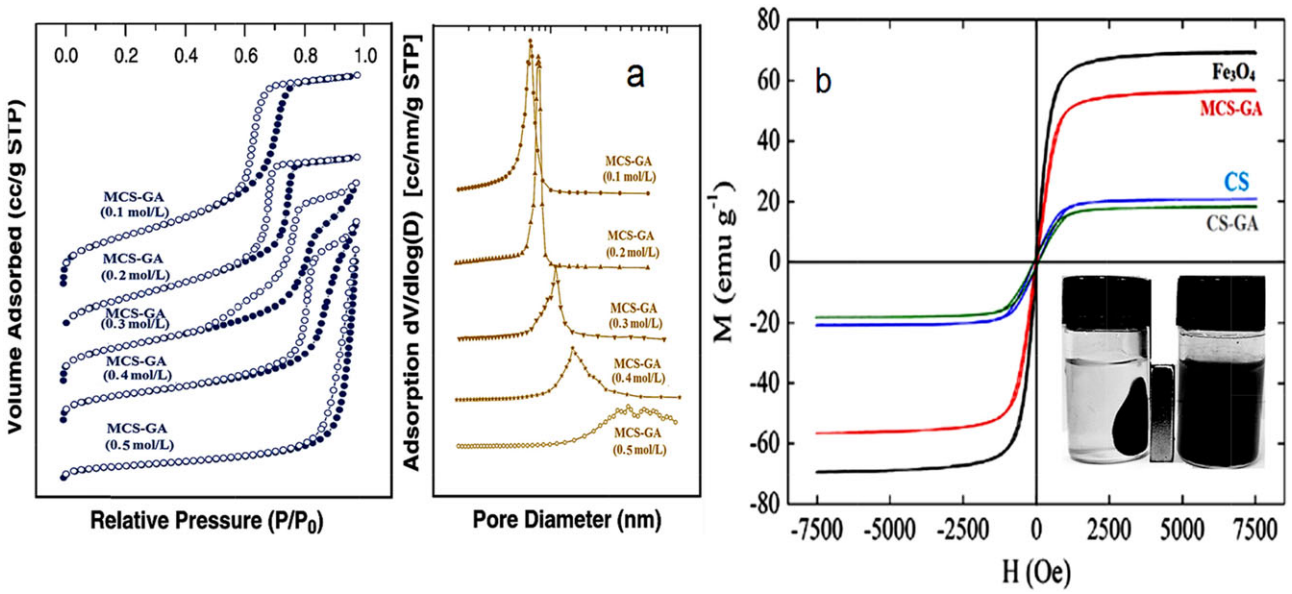

Figure 3. (a) N2 adsorption isotherms of MCS-GA with various GA contents; (b) VSM plot of CS and its modification.

attributed to the coating of magnetite (Fe_3O_4) nano-particles onto the surface of the CS-GA. In fact, these indicate that the Fe_3O_4 particles have a cubic inverse spinal structure with average size of 48 nm, based on the Debye–Scherrer equation.[23]

According to the EDX mapping images, the Fe particles loaded on the surface of chitosan (Fig. 2(b)) are well distributed. EDX analysis is used to determine the chemical composition of the MCS-GA before and after the adsorption process (Fig. 2(c) and 2(d)). Before the process, the elemental percentages of C, O, Fe and N atoms were 16.4, 26.27, 40.13 and 17.2, respectively. This indicates that the MCS-GA was successfully synthesized. After the adsorption process, three peaks which all occurred at around 19% were recorded along with the other major peaks, indicating appropriate adsorption of Hg (II) on the surface of magnetic chitosan modified with glutaraldehyde.

Transmission electron microscopy was used to analyze the particle morphology of MCS-GA (Fig. 2(e)). However, the MCS-GA consisted of multiple magnetite nanoparticles (Fe_3O_4) included in CS. Considering the results of the TEM micrograph, the structure of the synthesized adsorbent was non-uniform and had a sphere-like shape with size distribution ranging from 10 to 80 nm; it can be stated that these were distributed mostly around 50 nm. Furthermore, these results indicate that the structure of the synthesized adsorbent is core–shell type, and that tiny interspaces exist on the surface of the adsorbents causing the effective adsorption of Hg (II).

The magnetic property of MCS-GA was measured and presented through a VSM plot. As seen in Fig. 3(b), the VSM plot shows a value of 35.79 emu g^{-1}, which is close to the value reported for pure magnetite colloidal nanocomposite (36.941 emu g^{-1}); [24] this could be mainly due to the appropriate and abundant distribution of Fe_3O_4 loaded on CS. After the adsorption analysis, the magnetic modified composite was easily and rapidly separated from the treated sample using an external magnetic field. This implies that the magnetic properties of the adsorbent remained high enough for the magnetized separation process. As shown Fig. 1S, the brown particles were attracted to the vial immediately when in the presence of an external magnet, emphasizing the strong magnetic properties of the prepared adsorbent.

The N_2 sorption–desorption isotherms and pore size distribution of MCS-GA with different molar contents of GA are displayed in Fig. 3(a). As shown in this figure, all samples exhibit non-reversible adsorption–desorption isotherms; in other words, they have typical type IV isotherms according to the IUPAC classification. It is noteworthy that the shapes of the isotherms are in accordance with the GA molar ratio. A gradual change from H1-type to H2-type hysteresis loops at relatively high pressure was observed by increasing the GA molar content from 0.1 to 0.5. In addition, the MCS-GA 0.1 mol L^{-1}, MCS-GA 0.2 mol L^{-1} and MCS-GA 0.3 mol L^{-1} contain H1-type hysteresis loops with sharp condensation step at a P/P0 ratio of 0.50 to 0.7. The narrow distribution with relatively uniform pores (cylindrical pores) was observed to be characteristic of mesoporous MCS-GA, whereas the MCS-GA displayed semi H2-type hysteresis loops for other molar ratios. The latter contain more complex pore networks consisting of foam-like pore structures or voids between close-packed spherical particles and wide pore size distribution.

MCS-GA involves a wide pore size distribution, ranged from 1 nm to 100 nm, with two main parts in terms of size (i.e. a part at 0–10 nm and another part at 10–100 nm). Pore size distribution in size 0 to 10 nm is attributed to pores which could be formed by incorporating GA. Pore size distribution for the sizes 10 to 100 nm is assigned to the 1D morphology of the synthesized nanocomposites. This implies that the pores size expands from 16.21 to 27.31 and the BET specific surface area decreases from 482 to 343 m^2 g^{-1} when increasing the GA molar content from 0.5 to 1.5 (Table 4). The decreases in BET surface area could be due to the tight cumulated structure; also, the blocking effects of close-packed particles could be due to the low pore volume. Considering the above mentioned results, it can be said that the GA molar content strongly affects both the mesostructure and pore size of mesoporous MCS-GA.

Adsorption process

Effects of GA loading on MCS

According to the results, the Hg (II) adsorption capacity of the sorbent increases for high GA concentrations, Fig. 4. Previous studies suggest this could be attributed to the cross-linking reaction

Table 4. N2 adsorption–desorption results for various samples

Sorbent	Specific surface area ($m^2\ g^{-1}$)	Average pore diameter (nm)	Average pore volume ($cm^3\ g^{-1}$)
MCS	328	8.1	1.7
MCS-GA (0.25 mol L^{-1})	391	10.21	1.5
MCS-GA (0.5 mol L^{-1})	482	16.21	1.62
MCS-GA (1.0 mol L^{-1})	421	19.34	1.62
MCS-GA (1.5 mol L^{-1})	343	27.31	1.86

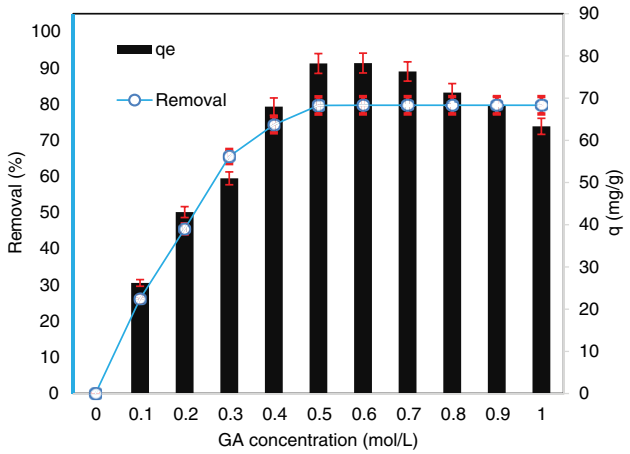

Figure 4. Impact of GA loading on Hg (II) removal efficiency (conditions: contact time 60 min, initial Hg (II) concentration 25 mg L^{-1} and temperature 20 °C).

between CS and GA (i.e. loading the GA on the surface of the MCS).[25] In addition, the capacity for adsorption of Hg (II) reached a maximum at a GA concentration of around 0.5 mol L^{-1}; in other words, the GA, which is used to form the synthesized adsorbent structure, starts to saturate at this stage resulting in less quaternary structure formation and limiting the Hg (II) adsorption capacity of the MCS-GA.

Effects of pH on the adsorption process

The pH plays an important role in the adsorption process due to its effects on metal ions in solution and the surface properties of the adsorbents (i.e. functional groups and surface charges). Therefore, the effects of pH on Hg (II) adsorption were investigated and results are shown in Fig. 5(a)). The lowest Hg (II) adsorption (36%) occurred at pH 2, and could be related to the competition between Hg (II) ions and protons (H^+). According to the results of previous studies, amino groups of CS are protonated at pH less than 5.0, which could induce electrostatic repulsion between Hg (II) and H^+. In addition, the adsorption capacity increased by 34% and 41% when pH reached 3 and 4, respectively.

At pH 5, the Hg (II) adsorption was further increased to 97.3%. Similarly, Zhou *et al.*[12] noted that the optimal sorption of mercury on modified magnetic crosslinking chitosan microspheres was obtained at pH 5. In addition, at pH >5, it can be seen that metal adsorption stabilized at 76%. However, with increases the pH of solution, the uptake efficiency dropped sharply. Therefore, the optimum pH for the solution is 5. This is mainly due to the presence of a free lone pair of electrons on N atoms in the MCS, which could be bonded and/or coordinated with the Hg (II) ions to give the corresponding resin–metal complex (Scheme 1). In addition, the presence of HCl in the medium leads to either the formation of $HgCl_2^-$ or another form of anion complex at pH 5. For the following reactions, $HgCl_2^-$ could exchange via the Cl^- which is electrostatically attached to the MCS-GA:

$$R\text{-}NH_2 + HCl \rightarrow R\text{-}NH_3^+Cl^- \quad (3)$$

$$HgCl_2 + Cl^- \rightarrow HgCl_3^- \quad (4)$$

$$R\text{-}NH_3^+Cl^- + HgCl_3^- \rightarrow R\text{-}NH_3^+HgCl_3^- + Cl^- \quad (5)$$

Moreover, Hg (II) ions turn to colloidal Hg $(OH)_2$ and separate from the solution phase at pH > 5. On the other hand, Hg (II) removal at this pH is attributed to the formation of an insoluble precipitate of metal hydroxide, which is not an adsorption process. The same trend was also reported for the sorption of mercury by magnetic chitosan resin modified with Schiff's base derived from thiourea and glutaraldehyde.[14]

Additionally, the point zero charge (PZC) of MCS-GA was determined using the solid addition method. As shown in Fig. 5(b), PZC for our adsorbent was 7.85, indicating that the synthesized adsorbent surface is positive at pH < 7.85, which is unfavorable for the adsorption of Hg (II) via electrostatic interaction. The adsorption capacity, even at pH 5, was observed to be about 75 mg g^{-1}; in other words, Hg (II) adsorption by MCS-GA in this form is related to the chelation interaction between Hg (II) and functional groups. It should be noticed that electrostatic interaction does not occur here, since, as mentioned above, MCS-GA is positively charged at pH < 7.85.

Contact time and kinetic

Figure 6 shows the efficiency of adsorption of Hg (II) by MCS-GA with initial concentrations of 25, 50, 75 and 100 mg L^{-1} at pH 5. During the first 15 min, the rate of adsorption of Hg (II) increased significantly, and then the magnetic modified composite gradually approached an equilibrium state. The initial rapid adsorption could be due to chemical binding, many vacant sites on the sorbent at the beginning of the process, or a high concentration gradient of Hg (II) in the solution.[26] Subsequently, vacant sites on the surface of the adsorbent became occupied by Hg (II) ions, reducing the concentration gradient as well as the adsorption efficiency.[27] Based on the results, it is obvious that increasing the initial concentration of Hg (II) from 25 to 100 mg L^{-1} enhanced the adsorption capacity from ~77 to ~135 mg g^{-1} and also decreased the removal percentage from 97.3% to 61%. The limited number of active sites and functional groups on the adsorbent surface increases the initial concentration of the adsorbate causing saturation of the adsorbent surface, thus decreasing the removal percentage. Increasing the gradient concentration along with initial concentration of the mercury improves the adsorption capacity.

The adsorption kinetics of Hg (II) was examined by applying several models, including pseudo-first-order, pseudo-second-order, intra-particle diffusion, Elovich, and fractional power kinetic. The parameters of the applied kinetic models and the regression correlation coefficients (R^2) which are used to describe the kinetics of Hg (II) are shown in Table 5. The R^2 values clearly indicate the best model is pseudo-second-order, with $R^2 > 0.996$ for all concentrations. In addition, the experimental q_e is also close to the calculated q_e value, leading to the conclusion that the mechanism

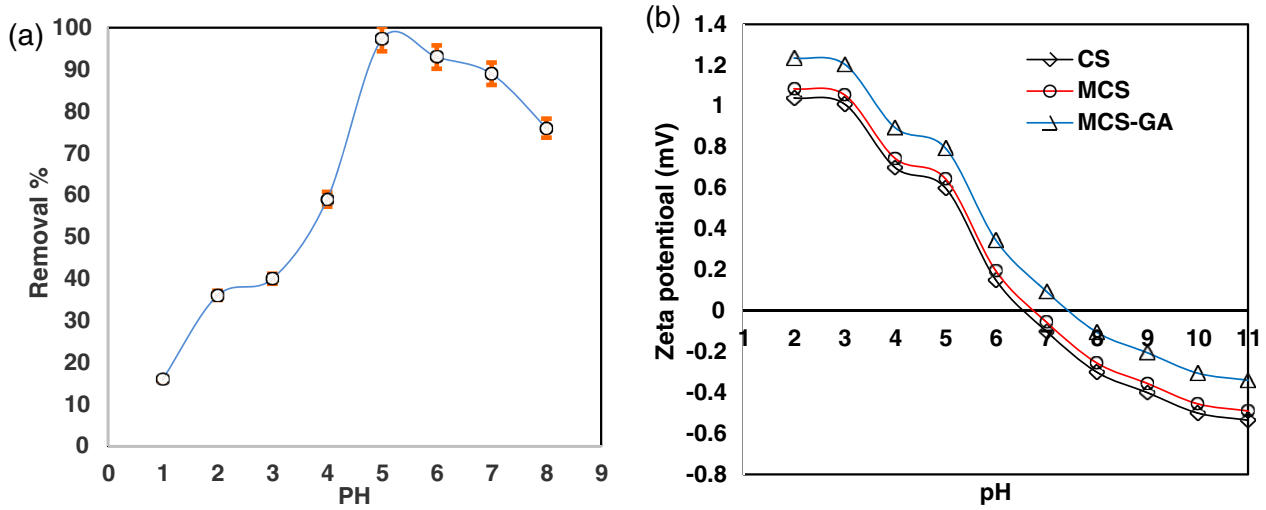

Figure 5. (a) Effects of pH on Hg (II) removal efficiency by MCS-GA composite (conditions: adsorbent dose 0.5 g L^{-1}, contact time 30 min, initial Hg (II) concentration 25 mg L^{-1} and temperature 20 °C). (b) Points of zero charge (pzc) determination for CS, MCS, and MCS-GA.

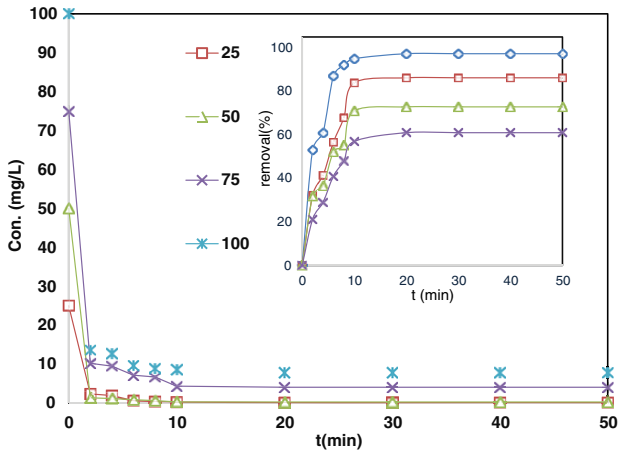

Figure 6. Effect of contact time (50 min) on the efficiency of removal of Hg (II) by MCS-GA composite (conditions: adsorbent dose 0.5 g L^{-1}, pH 5 and temperature 20 °C).

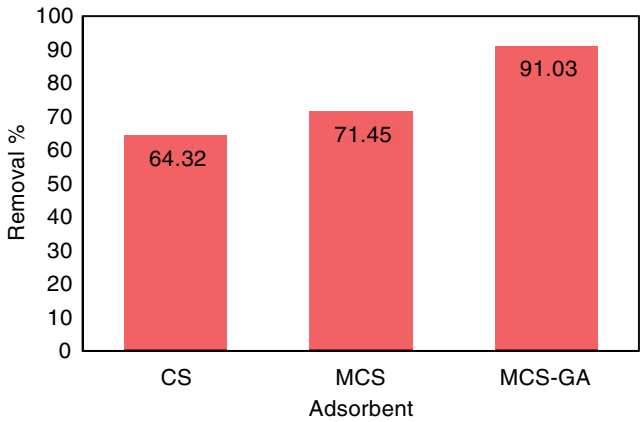

Figure 7. Adsorption efficiency of CS, MCS and MCS in actual wastewater.

of the adsorption process is pseudo-second-order. Similar observations were obtained for the adsorption of Hg (II) ions on poly (1-vinylimidazole)-grafted Fe_3O_4@SiO_2 magnetic nanoparticles and silica-multiwall carbon nanotubes thiol-functionalized polymer-coated magnetic particles.[4,28,29] It also indicates that the chemisorption reaction occurring with the amino groups on the surface of MCS-GA is rate-limiting and is the predominant rate controlling step.[30]

Considering the results presented in Table 1S, K_2 (the pseudo-second-order constant) decreased from 0.181 to 0.017 g mg^{-1} min when the growth initial ion concentration was between 25 and 75 mg L^{-1}. This also shows that the available active sites on the adsorbent swiftly become saturated by mercury ions, resulting in formation of the monolayer coverage of mercury on the surface of MCS-GA. Further results using the above mentioned models are presented in Table 2S.

Isotherms equilibrium

For an adsorption process it is important to define the equilibrium isotherms, since these isotherms explain the design of the adsorption system as well as the interactive behavior of Hg (II) ions and MCS-GA as the solid phase in this study. The distribution of Hg (II) between the liquid and solid phase was found to be in accordance with four isotherm models, namely, Langmuir, Freundlich, Dubinin–Radushkevich, and Temkin. The adsorption isotherms of Hg (II) onto the prepared adsorbent was studied using 25 mg L^{-1} initial mercury ion concentration, 1 g of the synthesized adsorbent at a temperature ranged from 25 to 45 °C, pH 5, and retention time of 15 min (Fig, 2S) .

However, the sharp slope which occurred at the beginning of the process in all isotherm curves indicated that the efficiency of the adsorbent is inversely related to the concentration of Hg (II). On the other hand, the efficiency of adsorbent is high at low Hg (II) concentration, while it decreases whenever the pollutant concentration increases. As also mentioned above, this is mainly due to the saturation of active sites on the adsorbent. Kunawoot Jainae *et al.*[29] obtained similar results for the adsorption of Hg (II) by thiol-functionalized polymer-coated magnetic particles. As shown in Table 6, the liner correlation coefficients (R^2) indicated that the Langmuir models (in which $R^2 > 0.981$) more closely describe the adsorption process at all temperatures, compared with the other models. The adsorption of Hg (II) thus occured on a homogeneous surface of MCS-GA by monolayer

Table 5. Comparison of adsorption capacity of Hg (II) between various modified CS found in the literature

Adsorbent	pH	q_{max} (mg g^{-1})	Isotherms	Ref.
MCS-GA (25 °C)	5	96	L	This work
Magnetic chitosan-thioglyceraldehyde	5.6	91	L	36
Aminated chitosan beads	4	89	L	37
Carboxymethyl-chitosan	6	281	F	38
Polymerization Calix[4]arene based chitosan polymer	6	74	L	39
Dihydroxy azacrown ether crosslinked chitosan (CCTS-AE)	5	22	L	40
Poly(ethyleneimine) grafted chitosan	5.8 ± .2	126	L	41

Table 6. The calculated thermodynamic parameters of the adsorption of Hg (II) by MCS-GA

	T (K)		Parameters		
Adsorbent		ΔG°	ΔH°	ΔS°	R^2
CS	294	−2.86	−18.23	+0.033	0.865
	303	−3.01			
	312	−3.74			
	322	−4.11			
	333	−4.98			
	334	−5.21			
		ΔG°	ΔH°	ΔS°	
MCS	294	−3.05	−16.67	+0.023	0.885
	303	−3.17			
	312	−3.98			
	322	−4.64			
	333	−5.10			
	334	−5.71			
		ΔG°	ΔH°	ΔS°	
MCS-GA	294	−3.59	−13.41	+0.010	0.943
	303	−3.87			
	312	−4.21			
	322	−4.93			
	333	−5.69			
	334	−6.11			

sorption, which is also in line with the results of the kinetic studies. Several researchers[31–33] reported monolayer sorption mechanisms for the sorption of Hg^{2+} ions onto different adsorbents. However, it should be considered that multilayer adsorption and heterogeneous distribution of active sites on adsorbent surface reflect the dominance of the Freundlich isotherm. As shown in Table 3S, the adsorption process is inherently exothermic; increasing the temperature decreases the equilibrium adsorption capacity (q_m). The q_m attenuation with increased temperature could be due to the degradation of chitosan structure expected at high temperatures.

The average adsorption energy (E) can be calculated using the Dubinin–Radushkevich isotherms, and E has been used in previous studies to predict the adsorption behavior.[34] Physical and chemical behaviors can be defined for E values <8 and >8 kJ mol^{-1}, respectively.[34] In this study the calculated E for Hg (II) indicated that the adsorption processes are predominantly chemisorption, which is strongly in accordance with the pseudo-second-order kinetics. The R_L is another important parameter in isotherm studies, and shows a suitable degree for the MCS-GA and its affinity toward Hg (II); in other words, $R_L > 1.0$, $R_L = 1$, $0 < R_L < 1$, and $R_L = 0$, indicate unfavorable, linear, suitable, and irreversible degrees, respectively. R_L, a non-dimensional parameter, is calculated using the Langmuir constant K_L (L/mg):

$$R_L = \frac{1}{1 + K_L C_\varepsilon} \tag{6}$$

The R_L value was between 0 and 1, indicating the suitability of Hg (II) adsorption by MCS-GA. This result was also confirmed by the values of Freundlich exponent '1/n', and also the Freundlich constant (K_F), since their values were $0 < 1/n < 1$ and $K_F > 5$, respectively, at all investigated temperatures.[35]

In order to assess the efficiency of the adsorbent synthesized in the present study, a comparative evaluation between the adsorbent used in the present work and other synthesis based chitosan adsorbents studied in the past is presented in Table 5. The q_m obtained for the Langmuir isotherm at room temperature was ~96 mg g^{-1}; in other words, the MCS-GA can be applied as a suitable adsorbent to remove Hg (II) ions as well as other heavy metals. It can be said that the appropriate adsorption capacity of Hg (II) results fom the existence of various functional groups, high surface area, and the size of sorbent particles. Moreover, from an economics point of view, the MCS-GA adsorbents are acceptable and can be easily separated from the treated solution using a magnetic field. Therefore, the MCS-GA developed in this work has high adsorption capacity and the potential for use in removing Hg (II) from polluted water and/or wastewater. Further information on the four isotherm models studied in this work is presented in Table 2S.

Adsorption thermodynamic

In this section, the interrelationship between temperature, entropy and enthalpy variables is assessed. The following Van't Hoff equation was used to assess the effect of temperature on

Table 7. Chloralkali wastewater characteristics

Characteristic	Value	Characteristic	Value
pH	5.7	K+	28.97 mg L^{-1}
TS	21 g L^{-1}	Mg2+	41.45 mg L^{-1}
TVS	320 mg L^{-1}	Zn2+	10 mg L^{-1}
EC	42.56 mS cm^{-1}	Fe2+	1.67 mg L^{-1}
Cl-	11300 mg L^{-1}	Mn2+	0.04 mg L^{-1}
Na+	8745 mg L^{-1}	Hg2+	345.21 mg L^{-1}

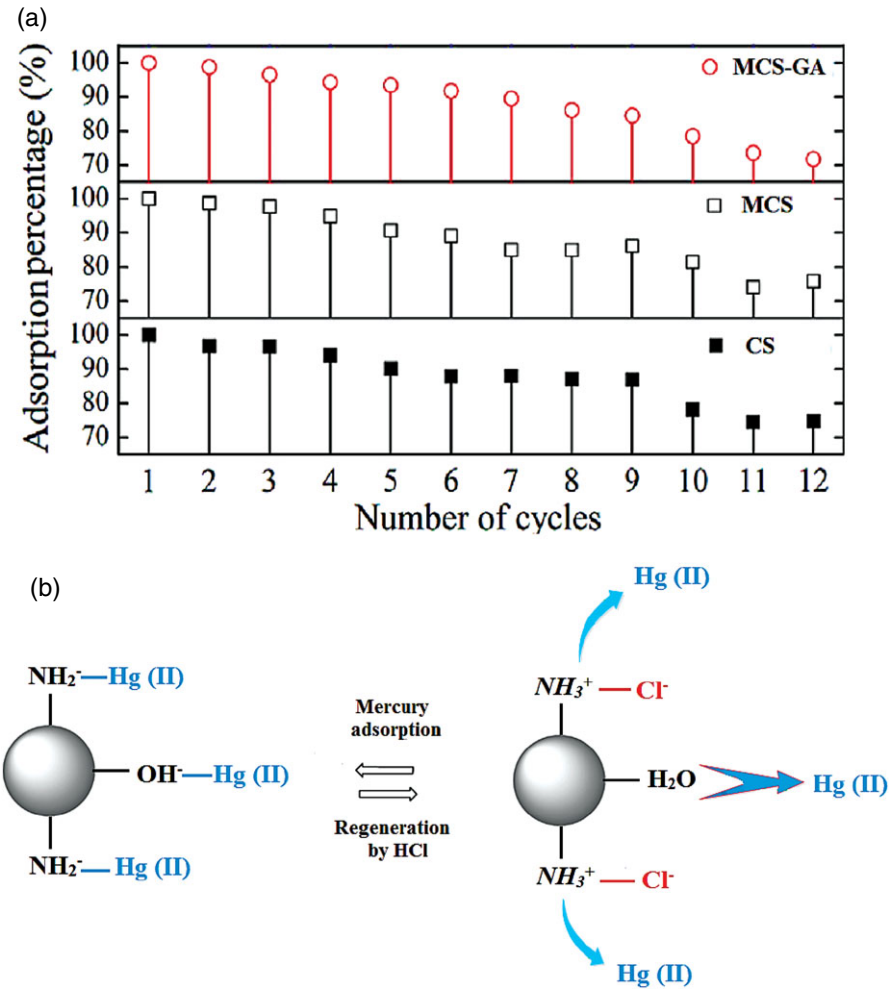

Figure 8. (a) The number of sorption–desorption cycles of Hg (II) on CS and modified CS. (b) Mechanism of the sorption–desorption process

the adsorption process and on the estimated thermodynamic parameters:

$$\ln k_c = \frac{\Delta S^0}{R} - \frac{\Delta H^0}{RT} \quad (7)$$

The constant K_c is defined as:

$$K_c = C_s/C_e \quad (8)$$

The values of enthalpy (ΔH^o, kJ mol^{-1}) and entropy (ΔS^o, kJ mol^{-1} K) were calculated from a linear plot of ln(K_c) versus 1/T and using the slope and intercept (figure not shown). The standard free energy (ΔG^o, kJ mol^{-1}) is linked to the changes of ΔH^o, ΔS^o, and temperature (T), according to the following equation:

$$\Delta G^0 = \Delta H^0 - (T\Delta S^0) \quad (9)$$

The above-mentioned thermodynamic parameters were calculated under steady-state reaction conditions and are shown in Table 6. The negative values of ΔG^o (−3.59 to −6.11) indicate that the adsorption of Hg (II) onto MCS-GA occurs spontaneously. However, the ΔG^o values decrease when the temperature is increased from 294 to 334 °C, indicating that the adsorption at lower temperatures is easier and more efficient, compared with other conditions: this was also found by Wang *et al.*[9] and Tran *et al.*[42]. However, Hadavifar *et al.* reported that physisorption happens at $0 < \Delta G^o > -20$, physisorption along with chemisorption occur at $-20 < \Delta G^o > -80$ and chemisorption alone is expected to occur at $-80 < \Delta G^o > -400$.[31] The mean value of ΔG^o in our study is −4.733; in other words, the interactions between mercury and MCS-GA have a physisorption mechanism, which is in contrast with the results of the isotherm and kinetic studies.[31]. According to the negative value of ΔH^o (−13.41) and also the reversed trend between ln (K_c) and temperature, the Hg (II) adsorption process is exothermic, while the MCS-GA has low affinity towards Hg (II) at higher temperature. When the ΔS^o value is positive (0.010), increasing randomness at the solid/solution interface during Hg (II) adsorption could be expected; besides, the positive ΔS^o value corresponds to a rise in the degree of freedom of the adsorbed species.[43] It has been speculated that the positive entropy reflects the ion replacement reactions because the release of the produced water molecules by ion exchange reactions between the Hg (II) and the functional groups of the MCS-GA could promote ΔS^o; in fact, positive ΔS^o in a system occurs whenever the ion releases from the solid surface to the solution.[31] The above observations were in accordance with previous studies.[9,44]

The adsorption efficiency under the real conditions

In order to survey the capability of CS, MCS, and MCS-GA to remove Hg (II) ions in the field, chloralkali wastewater was choose as a real case. Considering the optimized conditions obtained from the

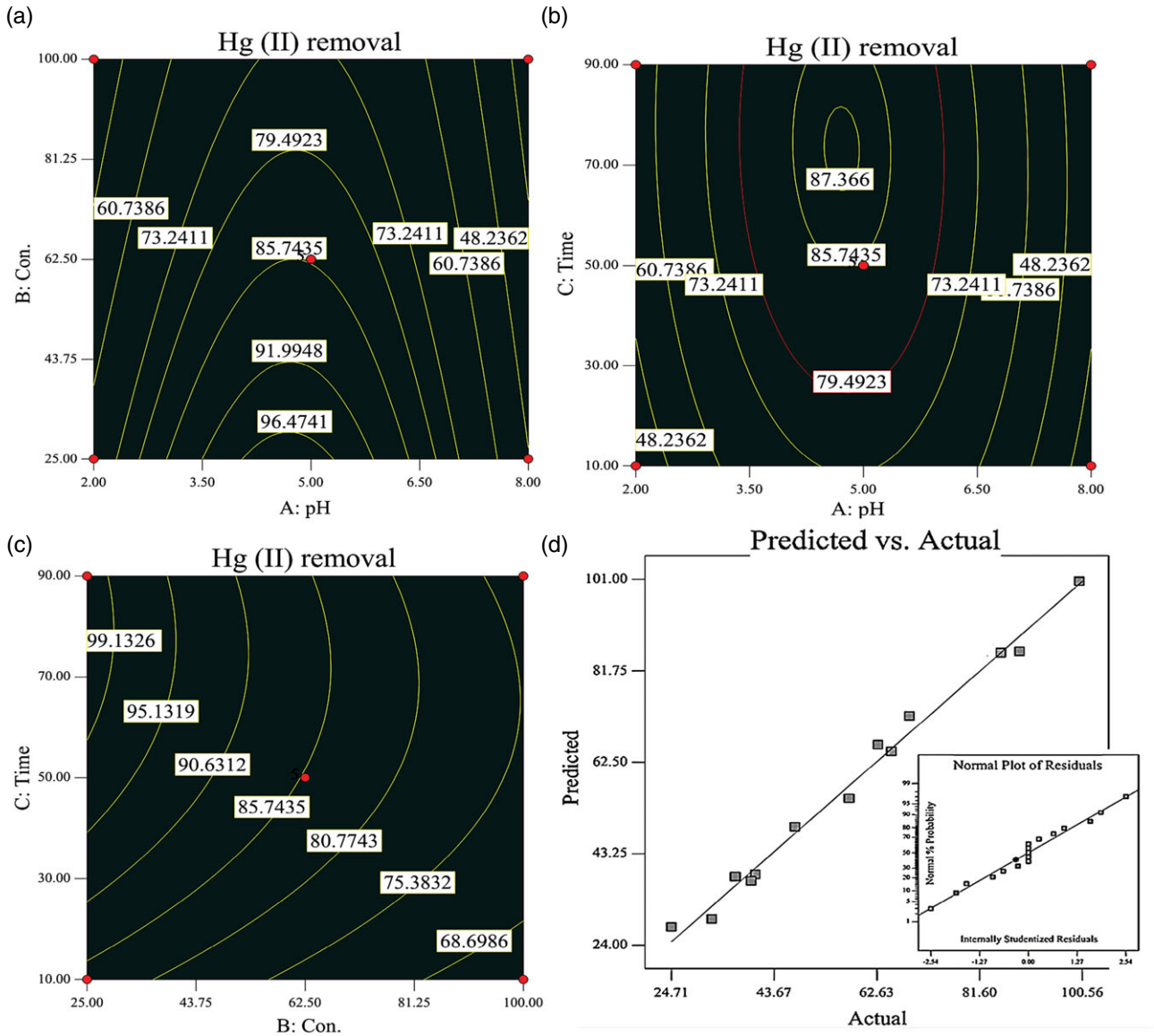

Figure 9. The interactive effect of (a) pH and initial concentration Hg^{2+}; (b) pH and contact time; and (c) initial concentration of Hg^{2+} and contact time on the removal efficiency. (d) Actual and predicted values of response for Hg^{2+} sorption on the MCS-GA and normal probability plot of the studentised residuals for adsorption process.

experiments on the synthesized wastewater, the Hg removal efficiency was investigated in real wastewater. The characteristics of chloralkali wastewater are listed in Table 7. As can be observed in this table, chloralkali wastewater contains high concentrations of various ions, which could restrict the adsorption process. Therefore, selecting the adsorbent should be considered a vital option. Figure 7 shows that MCS-GA is well able to adsorb Hg ions (91.03%) from chloralkali wastewater in comparison with other adsorbents.

Desorption studies

From a practical point of view, the regeneration of MCS-GA is essential to lower the costs and also make a user-friendly process of such an advanced adsorbent. Therefore, the separation of Hg (II) ions from the MCS-GA by hydrochloric acid was evaluated; the results are shown in Fig. 8(a). As shown in the figure, the desorption percentage of Hg (II) ions decreases slightly after 12 cycles, however, all the desorption ratios were >75%. Decreases in the removal efficiency could be due to the loss of MCS-GA during the several washing steps after each adsorption–desorption cycle. Moreover, it is possible that the active sites occupied by Hg (II) ions on the surface of the adsorbent were not completely recovered and/or regenerated by HCl desorption. The regeneration experiments firmly indicate that MCS-GA could be applied repeatedly as an efficient adsorbent for water/wastewater treatment. Desorption mechanisms of prepared adsorbent by HCl are shown in Fig. 8(b).

Hg (II) adsorption experiment design

A series of experiments based on a three-level BBD (Box–Behnken design) to optimize the adsorption conditions was performed. After running the experiments 17 times, the results obtained are shown in Table 4S and Fig. 9(c), (d), and (e).

Statistical analysis

Statistical analysis (ANOVA) was performed to evaluate the response of Hg (II) adsorption onto the MCS-GA. The results, given in Table 5S, showed that the response is a quadratic model (second-order). Also, the analysis showed that the *P*-values for the tested design are less than 0.0001, which proves that the selected design is highly significant. The predicted $R^2 > 0.929$ and adjusted $R^2 > 0.970$ also indicate that the model is significant.[7] Moreover, the impacts of other variable parameters were significant ($P < 0.05$) with 95% confidence levels, except for the second-order concentration ($P = 0.7623$). The R^2 for the model is 0.9869, which indicates that only ~1.31% of the independent variables cannot be explained by the regression design. The plot of actual and predicted values of Hg (II) adsorption is shown in Fig. 9(f), indicating that the developed design predicts the actual performance very well. .

An empirical relationship between the response (output) and the input variables can be obtained using BBD; also, the following fitted second-order model equation was used to express the relationship: (in coded units)

$$\text{Hg (II) removal} = 85.48 - 6.67A\ 11.67B + 6.23C + 1.98AB - 1.76\,AC - 2.05BC - - 10.27A^2 + 0.63B^2 - 5.50C^2 \quad (10)$$

In this equation, the negative and positive coefficients represent negative and positive effects on the Hg (II) adsorption process, respectively. The response could be improved by increasing the positive factors and reduced by increasing the negative factors. According to Equation (10), the C parameter (i. e. contact time) has a positive effect on Hg (II) removal, while A (pH) and B (initial concentration) parameters have negative effects. Considering that the highest coefficient belongs to the B (initial concentration), this factor has the greatest effect on the adsorption system, compared with the other independent parameters. The results of ANOVA showed that the initial concentration significantly affects Hg (II) removal ($P < 0.0001$). These results are in good agreement with previously reported results.[45]

CONCLUSION

In this work, the performance of a cross-linked CS with GA joined with magnetic nanoparticles (Fe_3O_4) for Hg (II) adsorption was evaluated. According to the results, the synthesized MCS-GA was found to have a fast adsorption rate. In addition, a decrease in q_{max} was observed for all concentrations when the temperature was raised. According to the thermodynamic analysis, the process occurs spontaneously, and has an exothermic nature with increasing randomness at the solid/liquid interface of the adsorption. The kinetic adsorption studies also showed that the adsorption system is pseudo-second-order with $R^2 > 0.996$. When assessing the selective absorption ability of MCS-GA, it was found that the modification process enhances the adsorption selectivity towards Hg (II) ions. Based on the results of the adsorption–desorption tests, the adsorbent demonstrates an efficient regeneration capacity for treating water/wastewater containing Hg (II) ions. The RSM indicated that the adsorption efficiency decreases when pH increases; and also, it was found that the initial concentration and contact time positively affect the adsorption process. It is suggested that pollution concentrations highly influence the adsorption of Hg (II) ions. Furthermore, the efficiency of the synthesized adsorbent was tested under real conditions. The results showed that MCS-GA is well able to adsorb Hg ions with a removal efficiency of 91.03% from chloralkali wastewater as a real wastewater.

Supporting Information

Supporting information may be found in the online version of this article.

REFERENCES

1 Caner N, Sari A and Tüzen M, Adsorption characteristics of mercury (II) ions from aqueous solution onto chitosan-coated diatomite. *Ind Eng Chem Res* **54**:7524–7533 (2015).
2 Pan S, Zhang Y, Shen H and Hu M, An intensive study on the magnetic effect of mercapto-functionalized nano-magnetic Fe_3O_4 polymers and their adsorption mechanism for the removal of Hg (II) from aqueous solution. *Chem Eng J* **210**:564–574 (2012).
3 Miretzky P and Cirelli AF, Hg (II) removal from water by chitosan and chitosan derivatives: a review. *J Hazard Mater* **167**:10–23 (2009).
4 Shan C, Ma Z, Tong M and Ni J, Removal of Hg (II) by poly (1-vinylimidazole)-grafted Fe 3 O 4@ SiO 2 magnetic nanoparticles. *Water Res* **69**:252–260 (2015).
5 Sinha A and Khare SK, Mercury bioremediation by mercury accumulating Enterobacter sp. cells and its alginate immobilized application. *Biodegradation* **23**:25–34 (2012).
6 Hadi P, To M-H, Hui C-W, Lin CSK and McKay G, Aqueous mercury adsorption by activated carbons. *Water Res* **73**:37–55 (2015).
7 Fakhri A, Investigation of mercury (II) adsorption from aqueous solution onto copper oxide nanoparticles: optimization using response surface methodology. *Process Safety Environ Protect* **93**:1–8 (2015).
8 Wang X, Yang L, Zhang J, Wang C and Li Q, Preparation and characterization of chitosan–poly (vinyl alcohol)/bentonite nanocomposites for adsorption of Hg (II) ions. *Chem Eng J* **251**:404–412 (2014).
9 Wang X, Sun R and Wang C, pH dependence and thermodynamics of Hg (II) adsorption onto chitosan-poly (vinyl alcohol) hydrogel adsorbent. *Colloids Surf A: Physicochem Eng Aspects* **441**:51–58 (2014).
10 Rabelo R, Vieira R, Luna F, Guibal E and Beppu M, Adsorption of copper (II) and mercury (II) ions onto chemically-modified chitosan membranes: equilibrium and kinetic properties. *Adsorption Sci Technol* **30**:1–22 (2012).
11 Ngah WW, Teong L and Hanafiah M, Adsorption of dyes and heavy metal ions by chitosan composites: a review. *Carbohydr Polym* **83**:1446–1456 (2011).
12 Zhou L, Liu Z, Liu J and Huang Q, Adsorption of Hg (II) from aqueous solution by ethylenediamine-modified magnetic crosslinking chitosan microspheres. *Desalination* **258**:41–47 (2010).
13 Wang J and Chen C, Chitosan-based biosorbents: modification and application for biosorption of heavy metals and radionuclides. *Bioresource Technol* **160**:129–141 (2014).
14 Donia AM, Atia AA and Elwakeel KZ, Selective separation of mercury (II) using magnetic chitosan resin modified with Schiff's base derived from thiourea and glutaraldehyde. *J Hazard Mater* **151**:372–379 (2008).
15 Younes I and Rinaudo M, Chitin and chitosan preparation from marine sources. structure, properties and applications. *Marine Drugs* **13**:1133–1174 (2015).
16 Roth H-C, Schwaminger SP, Schindler M, Wagner FE and Berensmeier S, Influencing factors in the CO-precipitation process of superparamagnetic iron oxide nano particles: a model based study. *J Magn Magn Mater* **377**:81–89 (2015).
17 Sargin İ and Arslan G, Effect of glutaraldehyde cross-linking degree of chitosan/sporopollenin microcapsules on removal of copper (II) from aqueous solution. *Desal Water Treat:* 1–13 (2015).
18 Rao KK, Chung I and Ha C-S, Synthesis and characterization of poly (acrylamidoglycolic acid) grafted onto chitosan and its polyelectrolyte complexes with hydroxyapatite. *React Funct Polym* **68**:943–953 (2008).
19 Lazaridis NK, Kyzas GZ, Vassiliou AA and Bikiaris DN, Chitosan derivatives as biosorbents for basic dyes. *Langmuir* **23**:7634–7643 (2007).
20 Yuwei C and Jianlong W, Preparation and characterization of magnetic chitosan nanoparticles and its application for Cu (II) removal. *Chem Eng J* **168**:286–292 (2011).
21 Zhou Y-T, Nie H-L, Branford-White C, He Z-Y and Zhu L-M, Removal of Cu 2+ from aqueous solution by chitosan-coated magnetic

nanoparticles modified with α-ketoglutaric acid. *J Colloid Interf Sci* **330**:29–37 (2009).
22 Vieira RS and Beppu MM, Dynamic and static adsorption and desorption of Hg (II) ions on chitosan membranes and spheres. *Water Res* **40**:1726–1734 (2006).
23 Travlou NA, Kyzas GZ, Lazaridis NK and Deliyanni EA, Functionalization of graphite oxide with magnetic chitosan for the preparation of a nanocomposite dye adsorbent. *Langmuir* **29**:1657–1668 (2013).
24 Li Y, Chu J, Qi J and Li X, An easy and novel approach for the decoration of graphene oxide by Fe 3 O 4 nanoparticles. *Appl Surf Sci* **257**:6059–6062 (2011).
25 Rosa S, Laranjeira MC, Riela HG and Fávere VT, Cross-linked quaternary chitosan as an adsorbent for the removal of the reactive dye from aqueous solutions. *J Hazard Mater* **155**:253–260 (2008).
26 Mohan D, Gupta V, Srivastava S and Chander S, Kinetics of mercury adsorption from wastewater using activated carbon derived from fertilizer waste. *Colloids Surf A: Physicochem Eng Aspects* **177**:169–181 (2001).
27 Azari A, Kakavandi B, Kalantary RR, Ahmadi E, Gholami M, Torkshavand Z *et al.*, Rapid and efficient magnetically removal of heavy metals by magnetite-activated carbon composite: a statistical design approach. *J Porous Mater* **22**:1083–1096 (2015).
28 Saleh TA, Isotherm, kinetic, and thermodynamic studies on Hg (II) adsorption from aqueous solution by silica-multiwall carbon nanotubes. *Environ Sci Pollut Res*: 1–11 (2015).
29 Jainae K, Sukpirom N, Fuangswasdi S and Unob F, Adsorption of Hg (II) from aqueous solutions by thiol-functionalized polymer-coated magnetic particles. *J Ind Eng Chem* **23**:273–278 (2015).
30 Boamah PO, Huang Y, Hua M, Zhang Q, Liu Y, Onumah J *et al.*, Removal of cadmium from aqueous solution using low molecular weight chitosan derivative. *Carbohydr Polym* **122**:255–264 (2015).
31 Hadavifar M, Bahramifar N, Younesi H and Li Q, Adsorption of mercury ions from synthetic and real wastewater aqueous solution by functionalized multi-walled carbon nanotube with both amino and thiolated groups. *Chem Eng J* **237**:217–228 (2014).
32 Arshadi M, Faraji A and Amiri M, Modification of aluminum–silicate nanoparticles by melamine-based dendrimer l-cysteine methyl esters for adsorptive characteristic of Hg (II) ions from the synthetic and Persian Gulf water. *Chem Eng J* **266**:345–355 (2015).
33 Zhang Y, Yan L, Xu W, Guo X, Cui L, Gao L *et al.*, Adsorption of Pb (II) and Hg (II) from aqueous solution using magnetic CoFe 2 O 4-reduced graphene oxide. *J Mol Liquids* **191**:177–182 (2014).
34 Zhou Z, Lin S, Yue T and Lee T-C, Adsorption of food dyes from aqueous solution by glutaraldehyde cross-linked magnetic chitosan nanoparticles. *Jf Food Eng* **126**:133–141 (2014).
35 Mouni L, Merabet D, Bouzaza A and Belkhiri L, Adsorption of Pb (II) from aqueous solutions using activated carbon developed from apricot stone. *Desalination* **276**:148–153 (2011).
36 Monier M, Adsorption of Hg 2+, Cu 2+ and Zn 2+ ions from aqueous solution using formaldehyde cross-linked modified chitosan–thioglyceraldehyde Schiff's base. *International journal of biological macromolecules* **50**:773–781 (2012).
37 Wang L, Xing R, Liu S, Cai S, Yu H, Feng J *et al.*, Synthesis and evaluation of a thiourea-modified chitosan derivative applied for adsorption of Hg (II) from synthetic wastewater. *Int J Biol Macromol* **46**:524–528 (2010).
38 Sun S and Wang A, Adsorption properties and mechanism of cross-linked carboxymethyl-chitosan resin with Zn (II) as template ion. *React Funct Polym* **66**:819–826 (2006).
39 Tabakci M and Yilmaz M, Synthesis of a chitosan-linked calix [4] arene chelating polymer and its sorption ability toward heavy metals and dichromate anions. *Bioresource Technol* **99**:6642–6645 (2008).
40 Yang Z, Zhuang L and Tan G, Preparation and adsorption behavior for metal of chitosan crosslinked by dihydroxy azacrown ether. *J Appl Polym Sci* **85**:530–535 (2002).
41 Zhou L, Liu S and Huang Q, Adsorption of mercury and uranyl onto poly (ethyleneimine) grafted chitosan microspheres. *Mod Chem Ind* **27**:175–177 (2007).
42 Tran L, Wu P, Zhu Y, Yang L and Zhu N, Highly enhanced adsorption for the removal of Hg (II) from aqueous solution by Mercaptoethylamine/Mercaptopropyltrimethoxysilane functionalized vermiculites. *J Colloid Interf Sci* **445**:348–356 (2015).
43 Kakavandi B, Kalantary RR, Farzadkia M, Mahvi AH, Esrafili A, Azari A *et al.*, Enhanced chromium (VI) removal using activated carbon modified by zero valent iron and silver bimetallic nanoparticles. *J Environ Health Sci Eng* **12**:115 (2014).
44 Raji F and Pakizeh M, Kinetic and thermodynamic studies of Hg (II) adsorption onto MCM-41 modified by ZnCl 2. *Appl Surf Sci* **301**:568–575 (2014).
45 Rahbar N, Jahangiri A, Boumi S and Khodayar MJ, Mercury removal from aqueous solutions with chitosan-coated magnetite nanoparticles optimized using the Box-Behnken design. *Jundishapur J Nat Pharmaceut Prod* **9** (2014).